

J

EGG--2105

Distribution DE91 015595

DISCLAIMER

This book was prepared as an account of work sponsored by an agency of the United States Government. Neither the United States Government nor any agency thereof, nor any of the employees makes any warranty, express or implied, assumes any legal liability or responsibility for the accuracy, completeness, or usefulness of any information, apparatus, product, or process disclosed, or represents that its use would not infringe privately owned rights. Reference herein to any specific commercial product, process, or service by trade name, trademark, manufacturer, or otherwise does not necessarily constitute or imply its endorsement, recommendation, or favoring by the United States Government or any agency thereof. The views and opinions of authors expressed herein do not necessarily state or reflect those of the United States Government or any agency thereof.

SURFACE-FINISH EFFECTS ON THE HIGH-CYCLE FATIGUE OF ALLOY 718

Gary E. Korth

Published June 1981

**EG&G Idaho, Inc.
Idaho Falls, Idaho 83415**

MASTER

ok
DISTRIBUTION OF THIS DOCUMENT IS UNLIMITED

Prepared for the
U.S. Department of Energy
Idaho Operations Office
Under DOE Contract No. DE-AC07-76IDO1570

DISCLAIMER

This report was prepared as an account of work sponsored by an agency of the United States Government. Neither the United States Government nor any agency Thereof, nor any of their employees, makes any warranty, express or implied, or assumes any legal liability or responsibility for the accuracy, completeness, or usefulness of any information, apparatus, product, or process disclosed, or represents that its use would not infringe privately owned rights. Reference herein to any specific commercial product, process, or service by trade name, trademark, manufacturer, or otherwise does not necessarily constitute or imply its endorsement, recommendation, or favoring by the United States Government or any agency thereof. The views and opinions of authors expressed herein do not necessarily state or reflect those of the United States Government or any agency thereof.

DISCLAIMER

Portions of this document may be illegible in electronic image products. Images are produced from the best available original document.

ABSTRACT

Load control high-cycle fatigue tests at 427 and 649°C were conducted on Alloy 718 specimens given various surface finishes. The standard surface preparation for fatigue specimens is a low-stress grind that minimizes the residual surface stresses. A low-stress grind surface was used for generating baseline data; other surfaces that could be considered feasible for large components fabricated in commercial shops were produced on test specimens, and the high-cycle fatigue strength of each was compared. Surface finishes produced by

belt sanding, grit blasting, fine machining, and electropolishing were examined. Surface roughness measurements were taken on typical specimens with each surface finish, and residual stress profiles were measured on three of the surface types. Results show little or no difference in fatigue life for the various surfaces; rather they indicate that residual stress profile and grain size are more important factors than surface roughness in determining high-cycle fatigue strength.

CONTENTS

ABSTRACT	ii
INTRODUCTION	1
MATERIALS	1
PREPARATION OF SPECIMENS AND SURFACE FINISHES	1
TEST DETAILS	4
RESULTS	6
DISCUSSION OF RESULTS	13
CONCLUSIONS	16
REFERENCES	17

FIGURES

1. Details of test specimens	3
2. Residual stress profiles of Alloy 718 fatigue specimens given various surface preparations	5
3. Optical comparator profile pictures of scratches in Alloy 718 fatigue specimens at their maximum depth	6
4. Scanning electron micrographs showing the various surface finishes	7
5. Scanning electron micrographs showing scratched specimens (a) before test, and (b) after failure	8
6. Effects of surface finish and grain size on high-cycle fatigue of Alloy 718 at 427°C	12
7. Surface finish effects on high-cycle fatigue of Alloy 718 tube at 649°C	12
8. Surface finish effects on high-cycle fatigue of Alloy 718 tube at 427°C	14
9. Residuals of curve fit of Alloy 718 tube data at 427°C	14
10. Surface finish effects on high-cycle fatigue of Alloy 718 plate at 427°C	15
11. Residuals of curve fit of Alloy 718 plate data at 427°C	15
12. Residuals of curve fit of Alloy 718 tube data at 649°C	16

TABLES

1. Chemistry, heat treatment, and grain size of Alloy 718 used in surface finish effects investigation	2
--	---

Surface roughness measurements typical of surface preparations	4
Details of shallow scratches in Alloy 718 fatigue specimens	6
Alloy 718 load control high-cycle fatigue data	8
Constants resulting from regression analysis of low-stress grind specimen data	13

SURFACE FINISH EFFECTS ON THE HIGH-CYCLE FATIGUE OF ALLOY 718

INTRODUCTION

Alloy 718 is a precipitation-hardening nickel-base superalloy that is being specified for various components for liquid-metal fast breeder reactors (LMFBRs). This alloy maintains high strength at elevated temperatures making it a desirable structural material. But the property that justifies most LMFBR applications is the alloy's resistance to thermal striping damage due to its high fatigue endurance strength. Thermal striping is a high-cycle fatigue phenomenon caused by thermal stresses from the fluctuating mixing action of sodium streams of differing temperatures impinging on the metal surfaces.

Most of the design data is generated from laboratory fatigue specimens with carefully controlled surface finishes prepared with a low-stress grind and buffed to a surface finish of 8-12 in. Since Alloy 718 has been shown¹ to be quite notch sensitive under cyclic loading, the detrimental effect on the high-cycle fatigue properties caused by shop surface finishes of actual components has been questioned. This report examines some of the surface finishes that could be produced in a commercial shop on an actual component. Limited tests were conducted with specimens given the following surface finishes: (a) belt-sanded; (b) grit-blasted; (c) fine lathe-turned; and (d) electropolished. The results were then compared with data from standard "low-stress grind-and-polish" laboratory fatigue specimens.

MATERIALS

All specimens used in this study were taken from the Alloy 718 Department of Energy reference heat (Ht. 2180-6-9458). Both 19.05-mm plate and 266.70-mm diameter x 9.53-mm wall seamless tube product forms were used. Chemistry, heat treatment, and grain size of Alloy 718 are listed in Table 1.

PREPARATION OF SPECIMENS AND SURFACE FINISHES

Test specimens taken from the 19.05-mm plate were fabricated into either axial or rotating bending specimens. Specimens cut from the seamless tube were machined into a different configuration of a rotating bending specimen. Details of all specimen types utilized are shown in Figure 1.

All specimens were in the age-hardened condition when the final surface finish was made. Also, all specimens were initially prepared with the low-stress grind surface and then either tested in that condition or altered to another surface condition. The details of various surface preparation are as follows:

1. Low-stress grind (baseline)

Work speed = 35 rpm
Wheel = 4A60J8VL
Linear velocity of wheel = 820 m/s
In feed = 0.00089 mm/rev.
Sparkout = 500 rev. (90 s)

2. Grit Blast

Grit #3 flint shot (dulled for 60 min)
Distance from nozzle = 100 mm
Air pressure = 415 kPa
Specimen rotation rate = 120 rpm
Coverage time = 60 s

3. Belt Sand

First paper = 120 grit
Second paper = 120 grit reversed

4. Electropolish

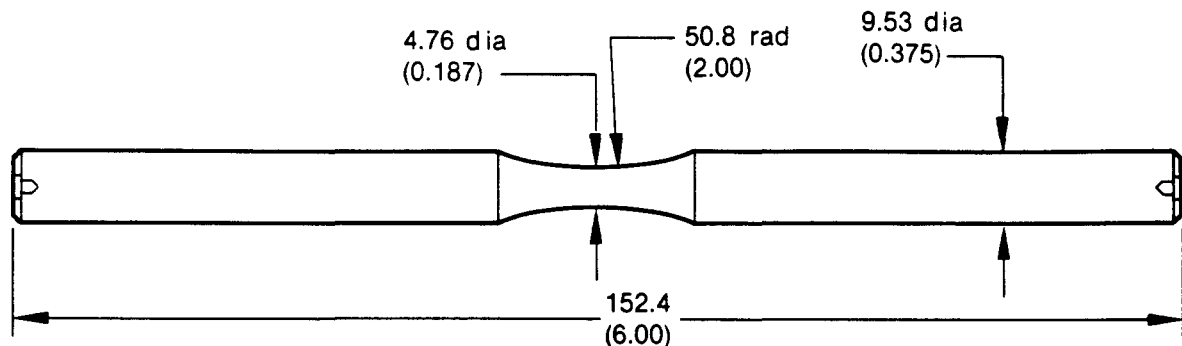
Removed approximately 0.075 mm of material from the radius of a low-stress grind specimen.

Solution: Ethylene glycol—74% (by vol.)
Sulfuric acid—25% (by vol.)
Hydrofluoric acid—1% (by vol.)

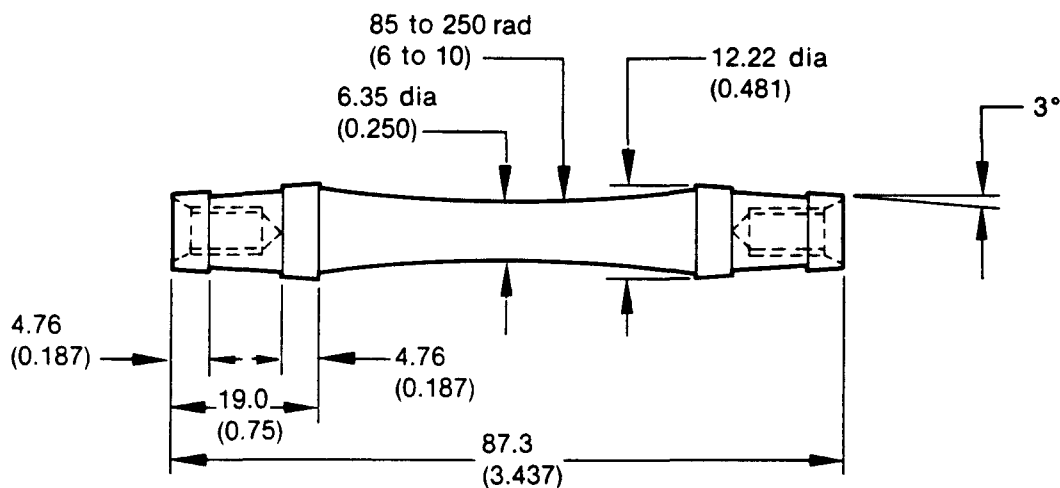
Table 1. Chemistry, heat treatment, and grain size of Alloy 718 used in surface finish effects investigation

Product Form ^a	Chemical Composition, weight %														
	Ni	Cr	Fe	Cb + Ta	Ti	Al	Mo	Co	Mn	Si	C	Cu	B	P	S
19.0 mm plate	Bal	18.22	19.29	5.17	0.98	0.64	3.04	0.06	0.10	0.19	0.05	0.08	0.002	0.005	0.002
26.7 mm OD x 9.7 mm wall tube	Bal	18.24	19.20	5.14	1.04	0.57	3.04	0.05	0.28	0.12	0.05	0.02	0.002	0.005	0.002
Heat Treatment															
Plate	954°C solution anneal 1 h, air cool, 718°C age for 8 h, furnace cool to 621°C, age for additional 8 h, air cool													6.8	
Tube	Same as plate except solution anneal temperature was 968°C													8.10	

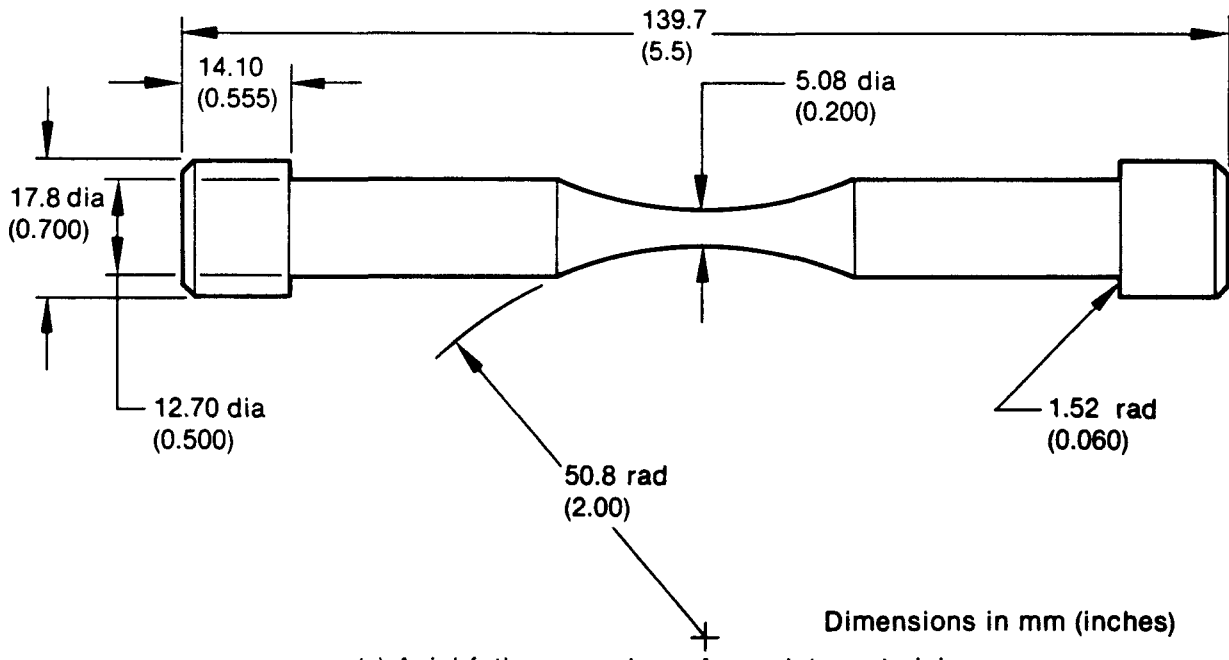
a Heat 2180-6-9458



(a) Rotating bending fatigue specimen from tube material



(b) Rotating bending fatigue specimen from plate material



(c) Axial fatigue specimen from plate material INEL-A-17 896

Figure 1. Details of test specimens.

Temperature—82°C
Current density—7.8 to 9.3 mA/mm²
Constant agitation
Series 300 stainless steel cathode

5. Lathe-Turned Machine Finish

Removed approximately 0.075 mm of material on a radius using fine precision cuts with cobalt-base high-speed tool steel. The tool bit was ground to conform to the hourglass radius so that all material was removed by plunge cutting rather than traverse turning.

The resulting surface roughness measurements taken from these various treatments are listed in Table 2.

Table 2. Surface roughness measurements typical of surface preparations

Surface Type	Surface Roughness (μ in. AA)
Low-stress grind	10
Grit blast	70
Belt sand	20
Electropolish	56
Lathe turn	12

Preparation of all test specimens taken from the seamless tube was performed by Metcut Research Associates, Inc., under subcontract. Metcut measured a residual stress profile on a typical specimen from each type of surface finish they prepared (low-stress grind, grit blast, and belt sand). The residual stress profile was measured by a technique involving a number of incremental steps using X-ray analysis and electropolishing. Further details and results of this technique are given in the report² issued by Metcut for their part of the study. The residual stress profiles for these three surface conditions are illustrated in Figure 2

which shows that the surface stress for the first 0.025 to 0.050 mm of depth is compressive for all three finishes.

The thickness of material removed during electropolishing and lathe turning from standard low-stress ground specimens was chosen to be 0.075 mm so that the effects of the previous surface would largely be removed. No actual residual stress profile measurements were taken on these last two surface preparations. However, previous investigations performed by Metcut for the Air Force on Alloy 718 have shown that electropolishing³ to a depth of 0.075 mm removes essentially all residual surface stress, leaving an almost zero-stress state, and that machine turning⁴ results in a profile very similar to those shown in Figure 2 except that the compressive stress persists to a greater depth.

Three other test specimens included in this study contained shallow circumferential scratches at the minimum diameter of the hourglass gauge section. These scratches were produced by a diamond stylus and ranged in depth from a visible indication only to 0.020 mm deep. The details of the shallow scratches are listed in Table 3. Two of the scratches were only part way around the circumference and varied in depth from zero to the maximum shown.

Optical comparator profile pictures of the two measurable scratches at their maximum depths are shown in Figure 3.

Scanning electron microscope (SEM) micrographs, typical of the five surface preparations used in this study, are shown in Figure 4, and two of the specimens with scratches are shown in SEM micrographs in Figure 5.

TEST DETAILS

The tests were conducted in either axial load control or rotating bending, utilizing specimens as shown in Figure 1. The waveform was sinusoidal and fully reversed (zero mean stress). All specimens were cycled in the fully elastic regime. The tests were conducted in an air environment using either induction heating techniques or a resistance enclosure furnace to obtain the elevated test temperature.

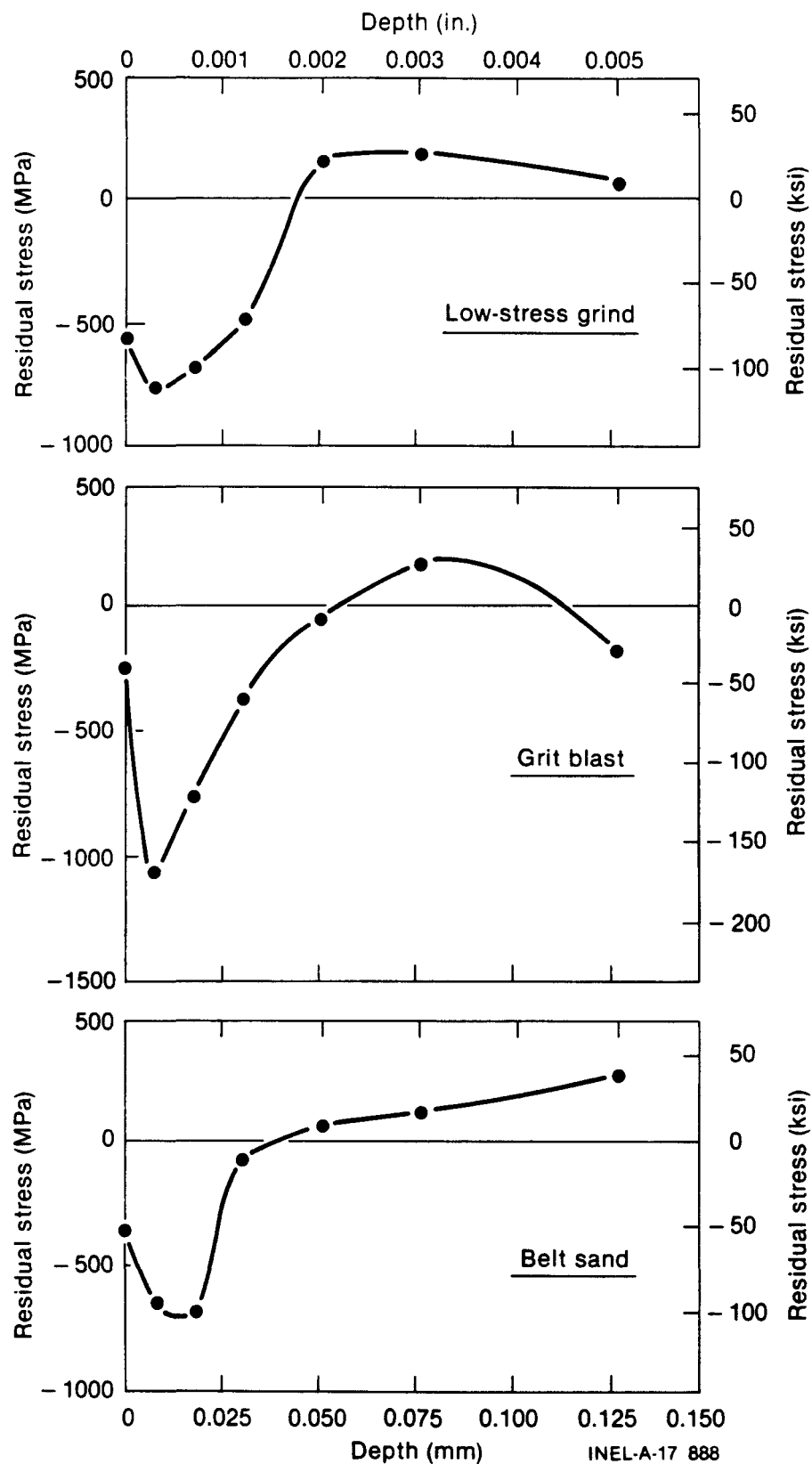
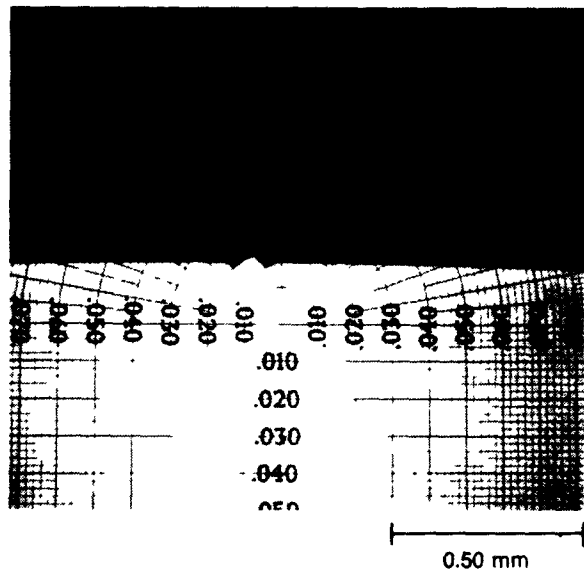


Figure 2. Residual stress profiles of Alloy 718 fatigue specimens given various surface preparations.

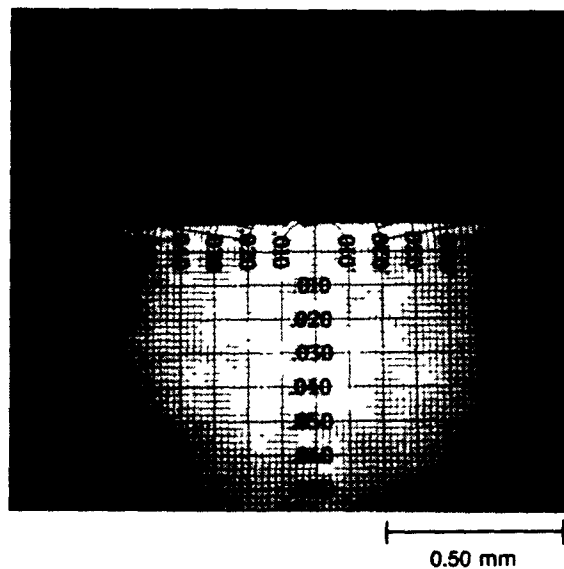
Table 3. Details of shallow scratches in Alloy 718 fatigue specimens

Specimen Number	Initial Surface State	Distance of Scratch Around Diameter (degrees)	Maximum Depth (mm)
R 21-12	Low-stress grind	180	0.020
R 24-13	Electropolished	270	0.010
R 21-3	Lathe-turned	360	— ^a

a. Visual indication only; scratch depth not measurable.



(a) Specimen R 21-12



(b) Specimen R 24-13

Figure 3. Optical comparator profile pictures of scratches in Alloy 718 fatigue specimens at their maximum depth.

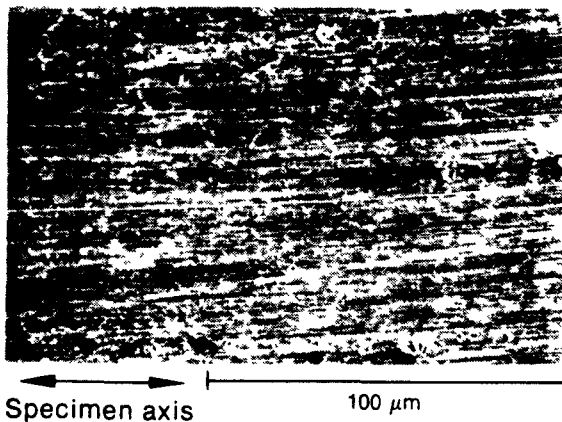
At 427°C both plate and tube low-stress grind specimens were tested. All the belt-sand and grit-blast specimens were from the tube material and all the electropolished and machine-turned specimens were from plate material. At the 649°C test temperature, all test specimens were taken from tube material.

RESULTS

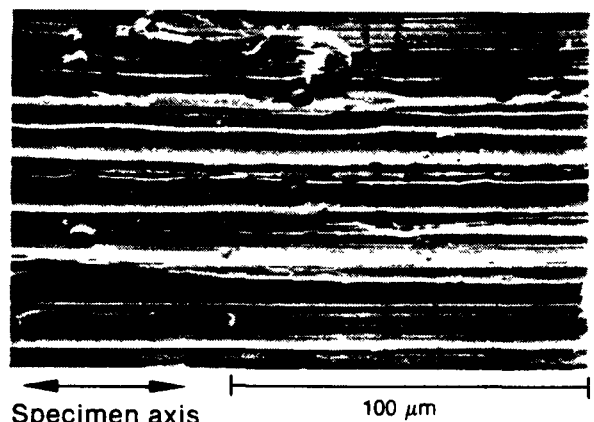
The test data from this investigation are listed in Table 4. Cycle life comparisons for the various

surface finishes are illustrated in Figure 6 for the 427°C tests and Figure 7 for the 649°C tests. The continuous curves shown on the figures were obtained from a regression analysis of the low-stress grind (baseline) data only. In the case of the 427°C tests, two different product forms of differing grain size were utilized in the investigation and therefore a curve for each grain size is shown. The equation used in the regression analysis was of the type:

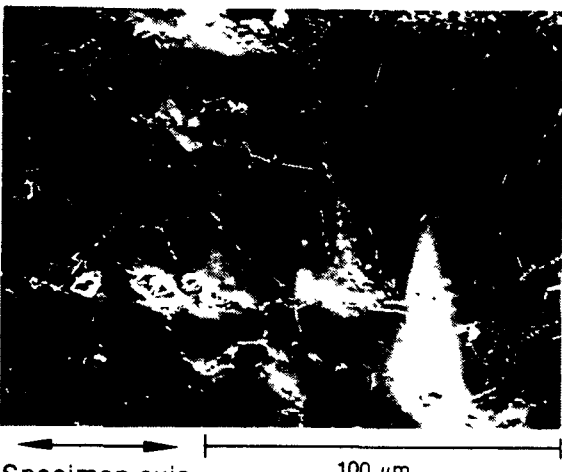
$$S_a = A N_f^Z + B \quad (1)$$



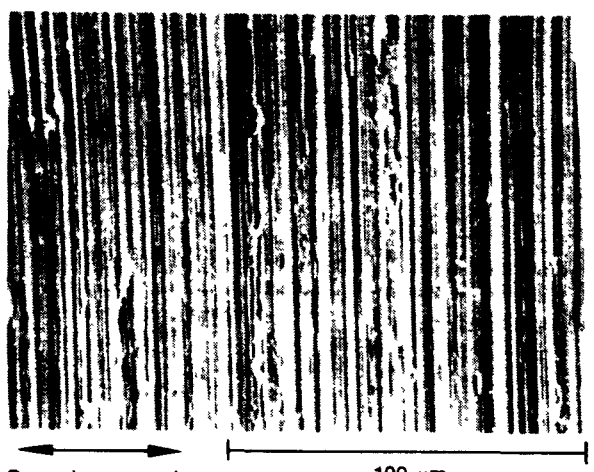
Specimen axis 100 μm
(a) Low-stress grind



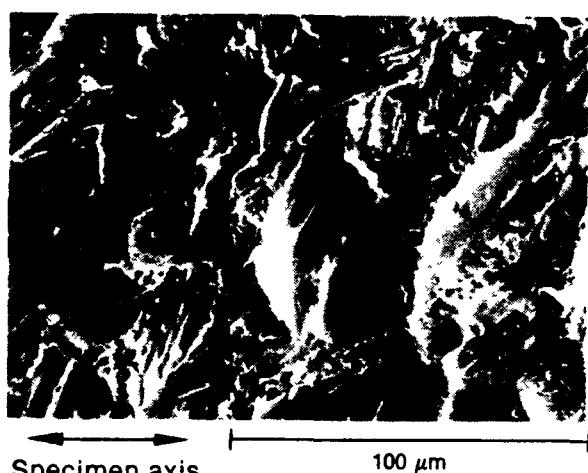
Specimen axis 100 μm
(b) Belt sand



Specimen axis 100 μm
(c) Electropolish



Specimen axis 100 μm
(d) Machine finish



Specimen axis 100 μm
(e) Grit blast

Figure 4. Scanning electron micrographs showing the various surface finishes.

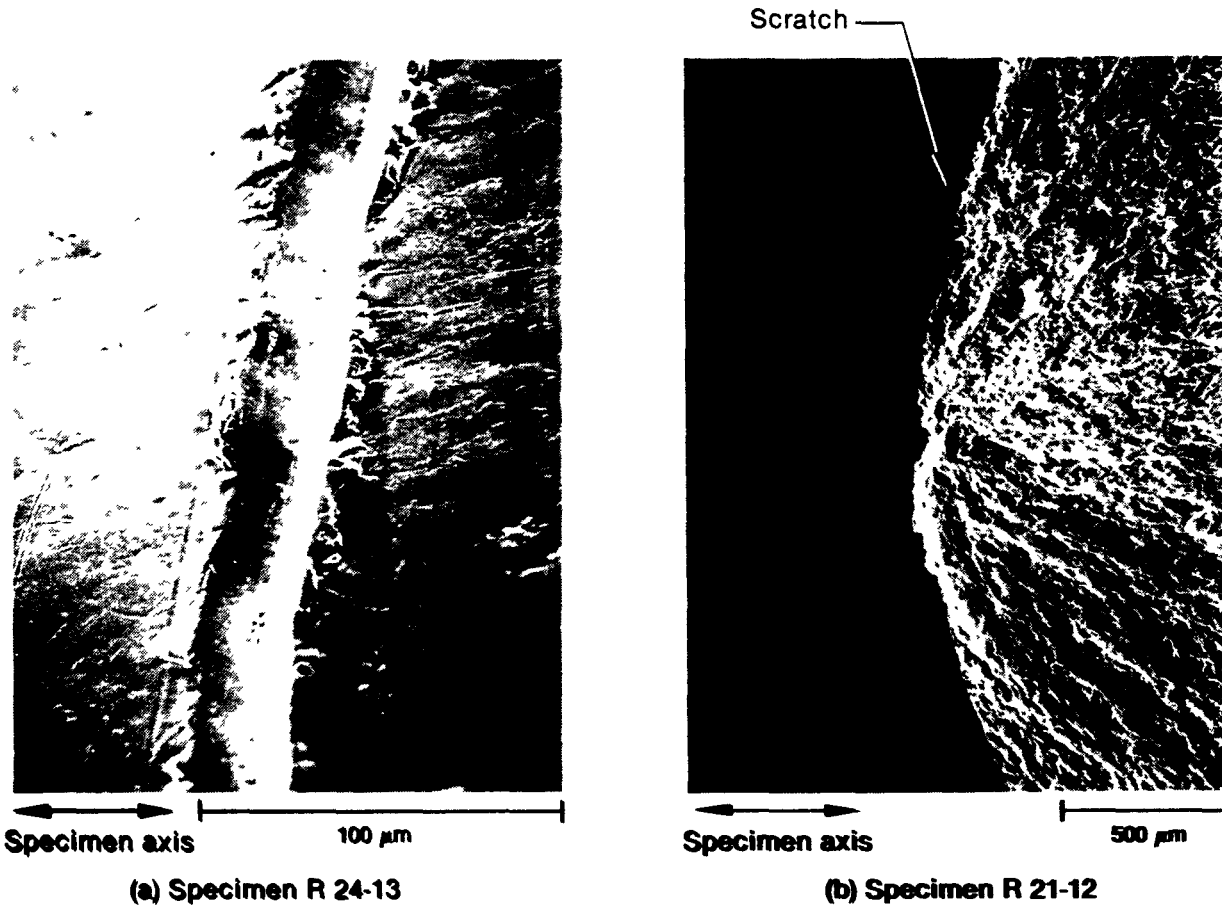


Figure 5. Scanning electron micrographs showing scratched specimens (a) before test, and (b) after failure.

Table 4. Alloy 718 load control high-cycle fatigue data

Specimen Number ^a	Test Temperature (°C)	Stress Amplitude (MPa)	Test Frequency (Hz)	Cycles to Fail, N_f	Type Test ^b	Surface Preparation ^c
RBM-6	427	754	125	180 000	RB	LSG
RBM-5	427	753	125	171 000	RB	LSG
R9-4	427	689	30	106 800	AX	LSG
RBM-3	427	670	125	509 000	RB	LSG
R9-5	427	655	30	227 100	AX	LSG
RBM-4	427	627	125	610 000	RB	LSG
R9-1	427	621	30	207 000	AX	LSG
R10-21	427	621	30	386 400	AX	LSG
RBM-8	427	615	125	1 284 000	RB	LSG
R10-32	427	610	30	377 800	AX	LSG
R10-36	427	603	30	674 000	AX	LSG
RBM-7	427	602	125	1 119 000	RB	LSG
R9-44	427	600	30	1 069 800	AX	LSG
R12-21	427	565	30	2 606 700	AX	LSG

Table 4. (continued)

Specimen Number ^a	Test Temperature (°C)	Stress Amplitude (MPa)	Test Frequency (Hz)	Cycles to Fail, N _f	Type Test ^b	Surface Preparation ^c
RB-65	427	552	167	1 222 000	RB	LSG
R12-3	427	552	40	2 138 700	AX	LSG
RBM-1	427	550	125	2 093 000	RB	LSG
RBM-2	427	546	125	9 704 000	RB	LSG
R12-24	427	538	10	3 118 700	AX	LSG
RB-70	427	538	167	16 077 000	RB	LSG
RP-97 ^d	427	521	20	1 551 710	AX	LSG
RB-66	427	517	167	79 719 000	RB	LSG
RBM-10	427	510	125	18 725 000	RB	LSG
RBM-9	427	498	125	6 006 000	RB	LSG
RBM-20	427	476	125	7 859 000	RB	LSG
R14-42	427	469	167	5 836 000	RB	LSG
RBM-19	427	469	125	13 178 000	RB	LSG
R15-26	427	455	167	21 414 000	RB	LSG
RB-64	427	455	167	197 325 000	RB	LSG
R14-22	427	448	167	4 498 000	RB	LSG
R15-55	427	438	167	8 772 000	RB	LSG
RP7-98 ^d	427	434	20	14 379 529	AX	LSG
R19-46	427	434	167	99 530 000	RB	LSG
R14-23	427	427	167	46 959 000	RB	LSG
R15-44	427	424	167	12 843 000	RB	LSG
R14-41	427	424	167	183 700 000 ^e	RB	LSG
R15-54	427	422	167	6 002 000	RB	LSG
R15-53	427	422	167	134 647 000	RB	LSG
R14-19	427	420	167	569 956 000 ^e	RB	LSG
R14-31	427	417	167	12 087 000	RB	LSG
R14-7	427	414	167	15 087 000	RB	LSG
R15-45	427	410	167	790 241 000 ^e	RB	LSG
RBM-68	427	761	125	148 000	RB	BS
RBM-69	427	758	125	152 000	RB	BS
RBM-70	427	681	125	391 000	RB	BS
RBM-73	427	663	125	615 000	RB	BS
RBM-59	427	610	125	888 000	RB	BS
RBM-58	427	610	125	987 000	RB	BS
RBM-60	427	556	125	3 269 000	RB	BS
RBM-56	427	532	125	2 281 000	RB	BS
RBM-65	427	516	125	5 313 000	RB	BS
RBM-61	427	516	125	18 080 000	RB	BS
RBM-76	427	483	125	34 971 000 ^e	RB	BS
RBM-75	427	455	125	7 317 000	RB	BS
RBM-27	427	758	125	150 000	RB	GB
RBM-29	427	745	125	122 000	RB	GB

Table 4. (continued)

Specimen Number ^a	Test Temperature (°C)	Stress Amplitude (MPa)	Test Frequency (Hz)	Cycles to Fail, N _f	Type Test ^b	Surface Preparation ^c
RBM-28	427	610	125	715 000	RB	GB
RBM-33	427	592	125	1 008 000	RB	GB
RBM-30	427	547	125	3 270 000	RB	GB
RBM-34	427	540	125	1 701 000	RB	GB
RBM-32	427	509	125	3 221 000	RB	GB
RBM-35	427	509	125	4 004 000	RB	GB
RBM-31	427	478	125	18 461 000	RB	GB
RBM-36	427	466	125	17 149 000	RB	GB
R24-18	427	517	30	2 281 252	AX	ELP
R24-16	427	496	30	2 109 893	AX	ELP
R24-10	427	469	30	1 771 134	AX	ELP
R24-3	427	469	30	2 302 230	AX	ELP
R14-29	427	455	167	338 996 000 ^e	RB	ELP
R14-16	427	448	30	106 401 520 ^e	AX	ELP
R9-3	427	414	30	25 409 098	AX	ELP
RP7-84 ^d	427	517	20	477 000	AX	MF
R3-38	427	517	20	556 700	AX	MF
RP7-85 ^d	427	517	20	569 200	AX	MF
R21-17	427	496	20	1 357 020	AX	MF
R21-4	427	455	20	3 218 900	AX	MF
R21-8	427	476	20	10 796 600	AX	MF
R24-13	427	448	20	20 458 000 ^e	AX	ELP ^f
R21-12	427	448	20	6 935 790	AX	LSG ^f
R21-3	427	469	20	2 584 880	AX	MF ^f
RBM-24	649	654	125	342 000	RB	LSG
RBM-23	649	649	125	342 000	RB	LSG
RBM-13	649	611	125	442 000	RB	LSG
RBM-14	649	601	125	664 000	RB	LSG
RBM-12	649	551	125	1 930 000	RB	LSG
RBM-18	649	550	125	1 318 000	RB	LSG
RBM-17	649	543	125	1 306 000	RB	LSG
RBM-11	649	538	125	7 540 000	RB	LSG
RBM-25	649	531	125	30 018 000 ^e	RB	LSG
RBM-26	649	522	125	8 046 000	RB	LSG
RBM-15	649	517	125	30 672 000 ^e	RB	LSG
RBM-16	649	512	125	10 197 000	RB	LSG
RBM-72	649	687	125	269 000	RB	BS
RBM-71	649	677	125	192 000	RB	BS
RBM-63	649	654	125	187 000	RB	BS
RBM-62	649	649	125	741 000	RB	BS
RBM-52	649	625	125	836 000	RB	BS
RBM-54	649	621	125	550 000	RB	BS

Table 4. (continued)

Specimen Number ^a	Test Temperature (°C)	Stress Amplitude (MPa)	Test Frequency (Hz)	Cycles to Fail, N _f	Type Test ^b	Surface Preparation ^c
RBM-55	649	538	125	2 919 000	RB	BS
RBM-53	649	523	125	5 947 000	RB	BS
RBM-57	649	522	125	10 363 000 ^e	RB	BS
RBM-64	649	515	125	3 137 000	RB	BS
RBM-74	649	483	125	54 641 000 ^e	RB	BS
RBM-77	649	481	125	8 106 000	RB	BS
RBM-43	649	689	125	91 000	RB	GB
RBM-42	649	677	125	53 000	RB	GB
RBM-46	649	649	125	383 000	RB	GB
RBM-44	649	642	125	411 000	RB	GB
RBM-40	649	602	125	841 000	RB	GB
RBM-38	649	583	125	1 161 000	RB	GB
RBM-49	649	547	125	2 965 000	RB	GB
RBM-39	649	532	125	4 098 000	RB	GB
RBM-37	649	526	125	2 715 000	RB	GB
RBM-48	649	516	125	4 956 000	RB	GB
RBM-47	649	515	125	14 569 000	RB	GB
RBM-45	649	483	125	19 193 000	RB	GB
RBM-41	649	481	125	16 833 000	RB	GB

a. Specimen Number: RBM-XX = ref. heat (2180-6-9458) 267-mm dia. x 9.5-mm wall tube, all others-XX = ref. heat (2180-6-9458) 19-mm plate. All specimens were solution annealed at 954-968°C for 1 h and duplex age hardened at 718°C for 8 h, furnace cooled to 621°C, and held for total aging time of 18 h.

b. AX = axial test; RB = rotating beam test.

c. Surface preparation: LSG = low-stress grind, BS = belt-sand, GB = grit blast, ELP = electropolish, MF = machine finish.

d. Uniform gauge specimen; all others hourglass.

e. Test terminated; specimen did not fail.

f. Contained scratch in gauge; see Table 3 for details.

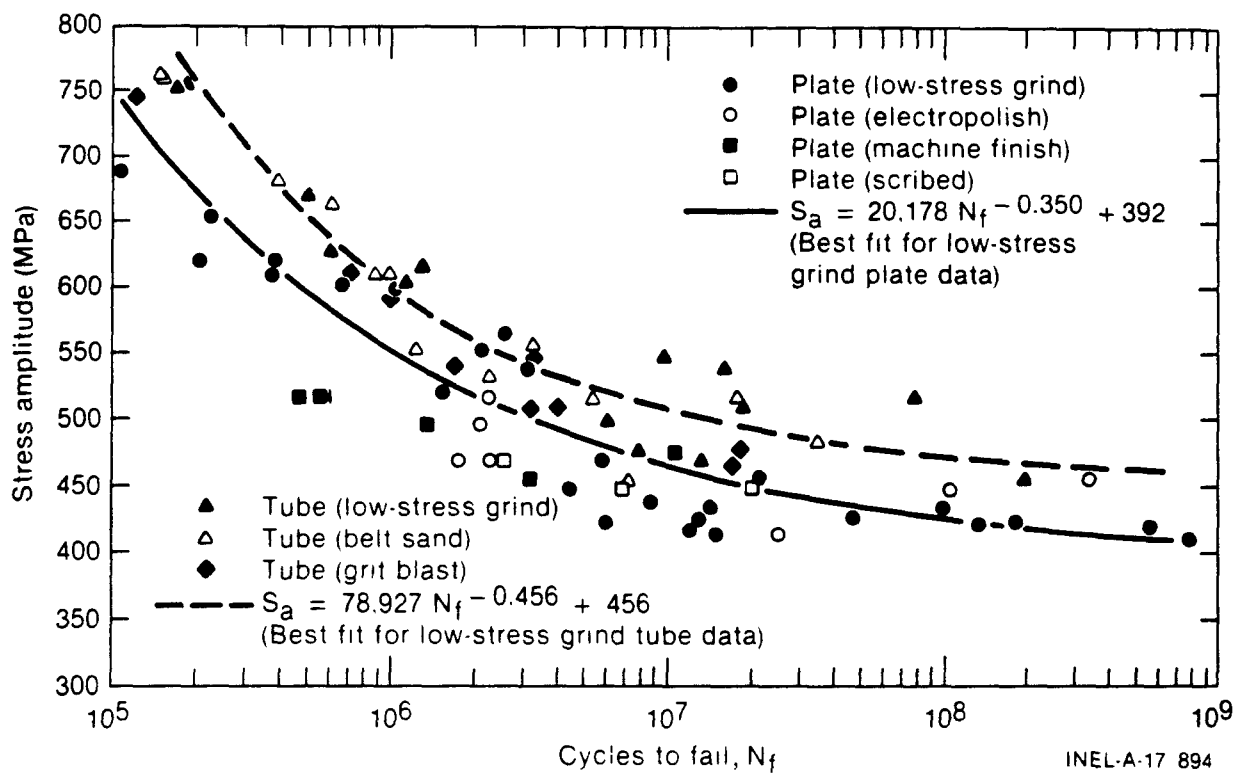


Figure 6. Effects of surface finish and grain size on high-cycle fatigue of Alloy 718 at 427°C.

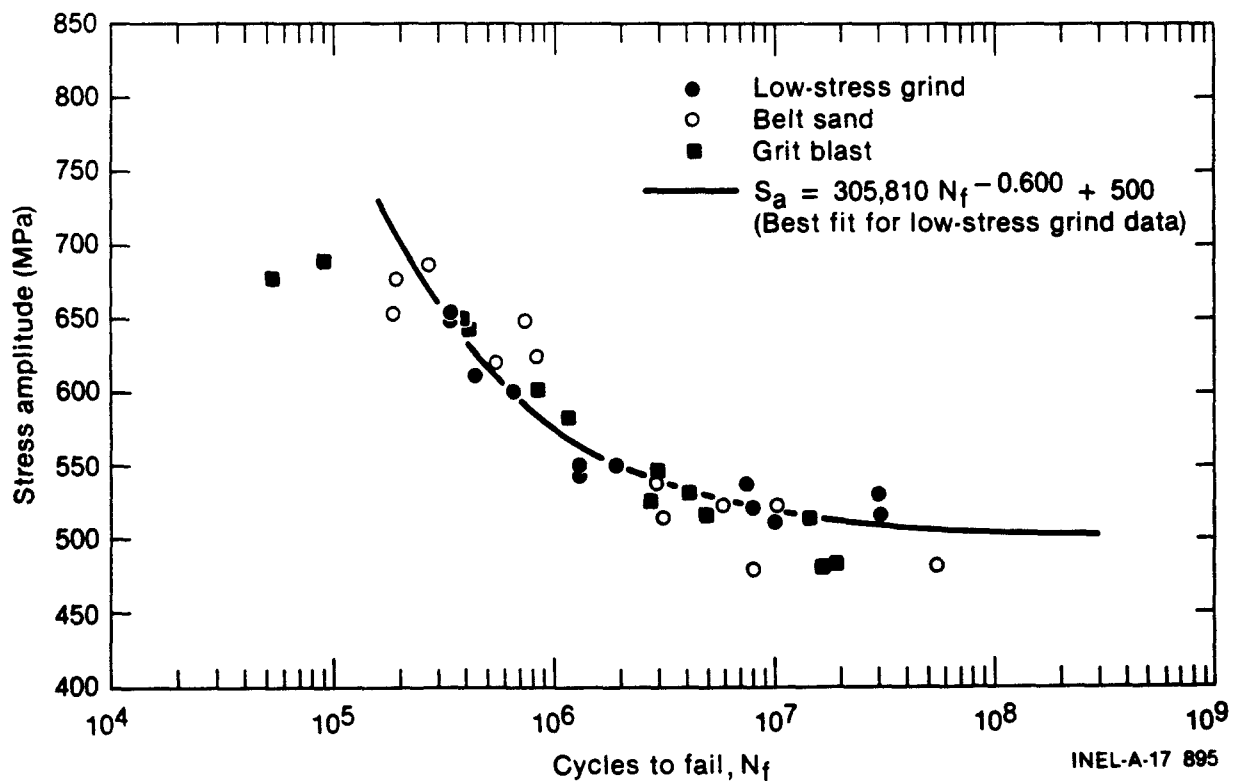


Figure 7. Surface finish effects on high-cycle fatigue of Alloy 718 tube at 649°C.

where

S_a = stress amplitude in MPa

N_f = cycles to failure

A, Z, and B are constants.

The constants obtained from the best-fit analysis are listed in Table 5.

DISCUSSION OF RESULTS

Before the effect of surface finishes can be evaluated, the effect of grain size must be accounted for. Two product forms were utilized in this investigation: 19-mm thick plate and 267-mm OD x 9.5-mm wall roll-extruded tube. The plate material exhibited a grain size of ASTM 7-8 and the grain size of the tubing was ASTM 8-10. Grain size has been shown⁵ to affect high-cycle fatigue of Alloy 718 and appears to be a more dominant factor than the surface finishes examined. Therefore, to evaluate surface finish effects, only product forms with similar grain sizes were compared.

Figure 8 shows the 427°C tube data comparing the low-stress grind, belt-sand, and grit-blast surfaces. The best fit curve determined for the low-stress grind (baseline) data is shown in Figure 8. Figure 9 is a residuals^a vs cycles-to-fail plot that enhances any differences in fatigue behavior between the baseline surface (low-stress grind) and the other two surfaces. These two figures illustrate

a. Residual = (S_a) calculated - (S_a) observed.

that there is no observable difference beyond normal data scatter in the fatigue life among the three surface finishes examined.

Figures 10 and 11 show the 427°C plate data and residuals plot, respectively. In this case, low-stress grind surfaces are compared to machine finishes, electropolished surfaces, and shallow-scratched surfaces. Again little difference in the fatigue life is noted among the different surface finishes. The lathe-turned machined finish appears to have a slight detrimental bias in the 5×10^5 to 5×10^6 cycle life regime, but at higher cycle lives its behavior is equivalent to that of the other surfaces. Even the scratched specimens did not appear to be unduly affected in their high-cycle fatigue behavior.

It is believed that the state of residual surface stress, and not surface roughness, is the dominant factor in governing high-cycle fatigue strength. This same conclusion was apparent from the Metcut studies^{3,4} with Alloy 718. Another experimental study,⁶ in which En 31 steel (1 C-1.5 Cr type steel) was fatigue tested with various surface grinding techniques, also concluded that residual stress and not surface roughness is the dominating factor. The residual stress profiles of low-stress grind, belt-sand, grit-blast, and fine lathe-turned surface preparation techniques all produced similar moderate compressive stresses at, and slightly below the surface; all specimens with these surfaces exhibited similar high-cycle fatigue behavior. There is, however, an unresolved point in the case of the electropolished specimens. They were believed to have had a near-zero residual surface stress even though no actual measurements were performed on the specimens after electropolishing. A previous investigation³ cited earlier showed that flat 1.65-mm specimens which were heat

Table 5. Constants resulting from regression analysis of low-stress grind specimen data

Test Temperature (°C)	Product Form	A	B	Z
427	Plate	20,178	392	-0.350
427	Tube	78,927	456	-0.456
649	Tube	305,810	500	-0.600

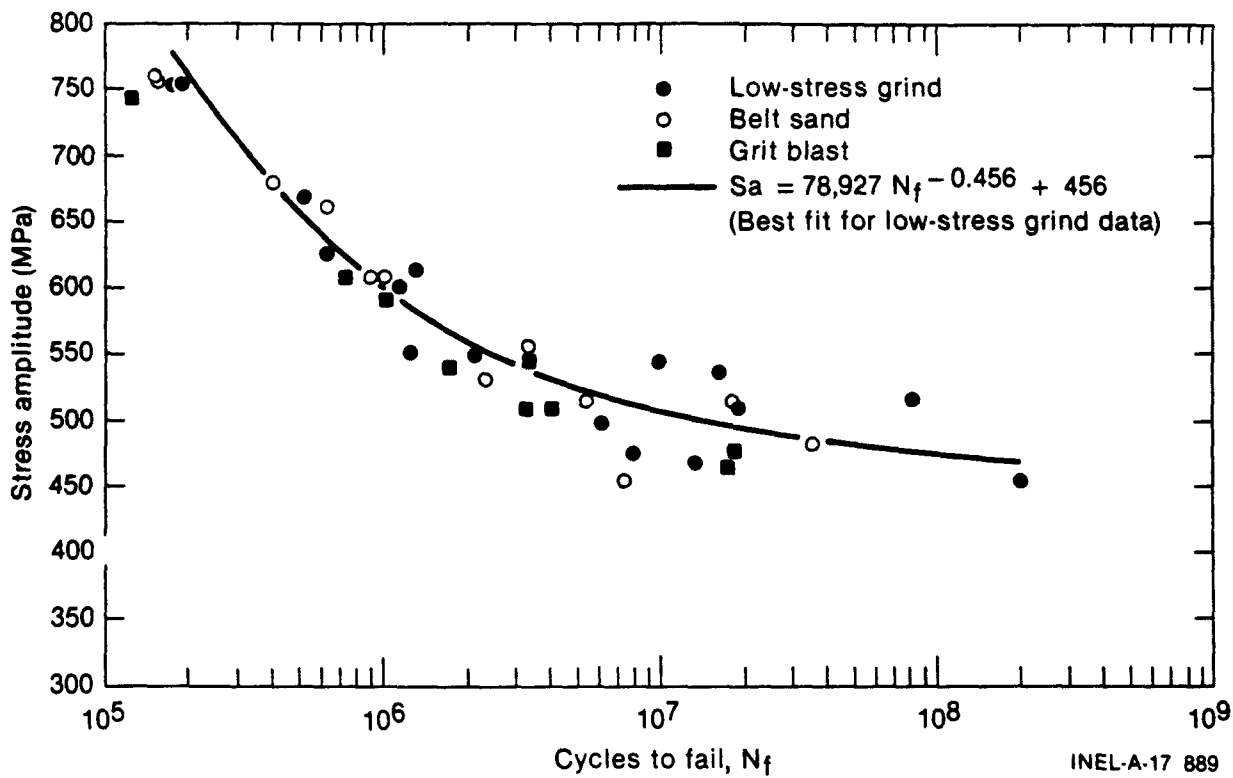


Figure 8. Surface finish effects on high-cycle fatigue of Alloy 718 tube at 427°C.

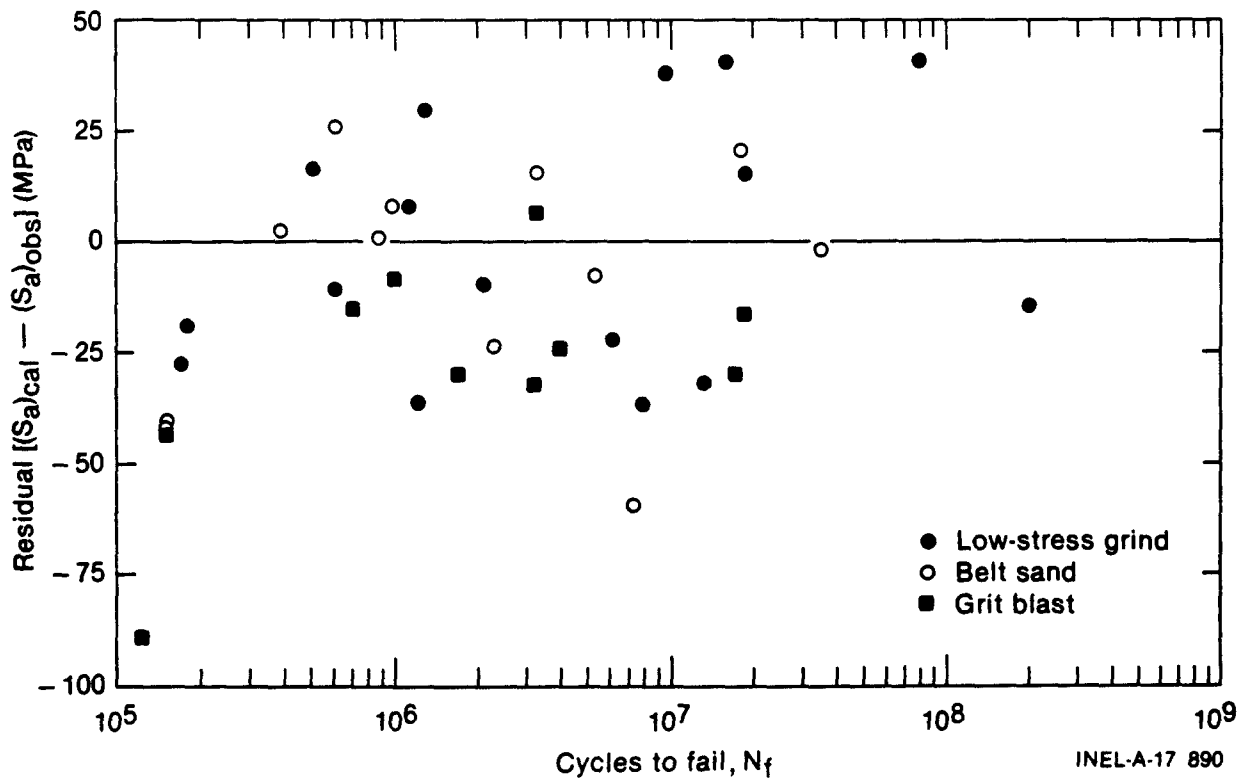


Figure 9. Residuals of curve fit of Alloy 718 tube data at 427°C.

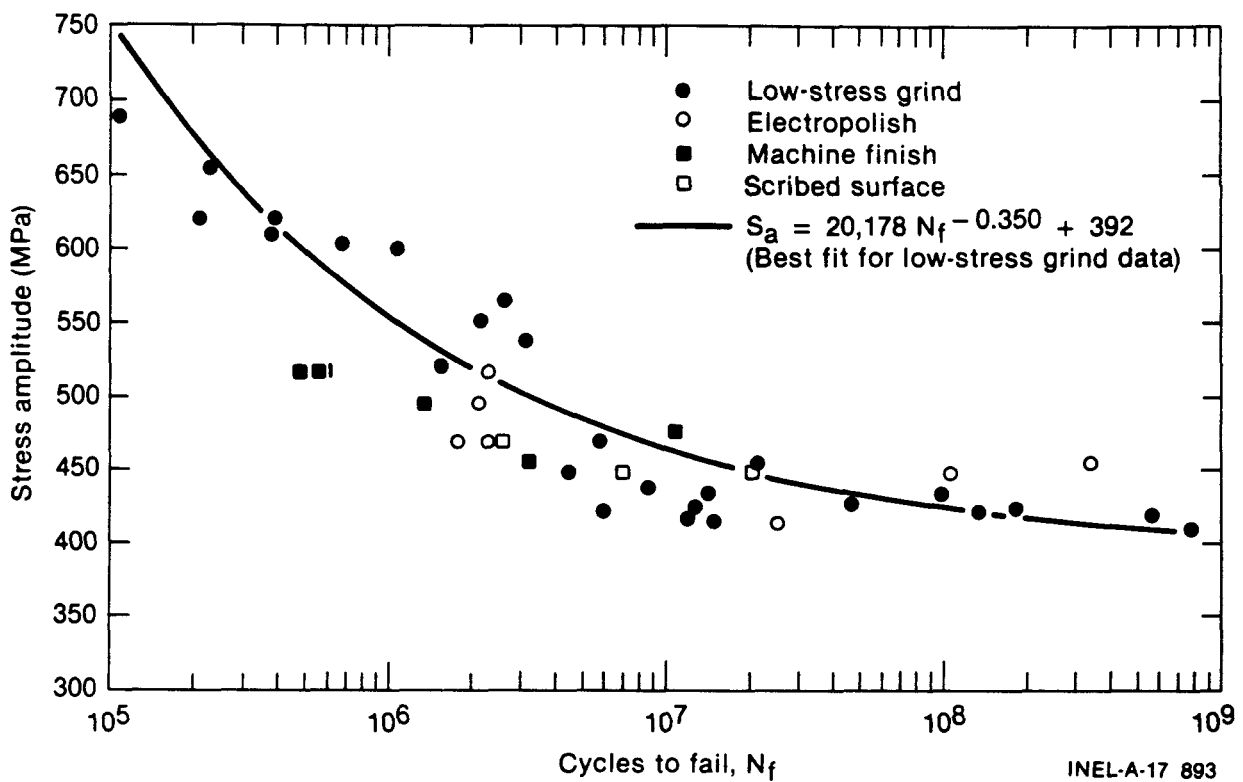


Figure 10. Surface finish effects on high-cycle fatigue of Alloy 718 plate at 427°C.

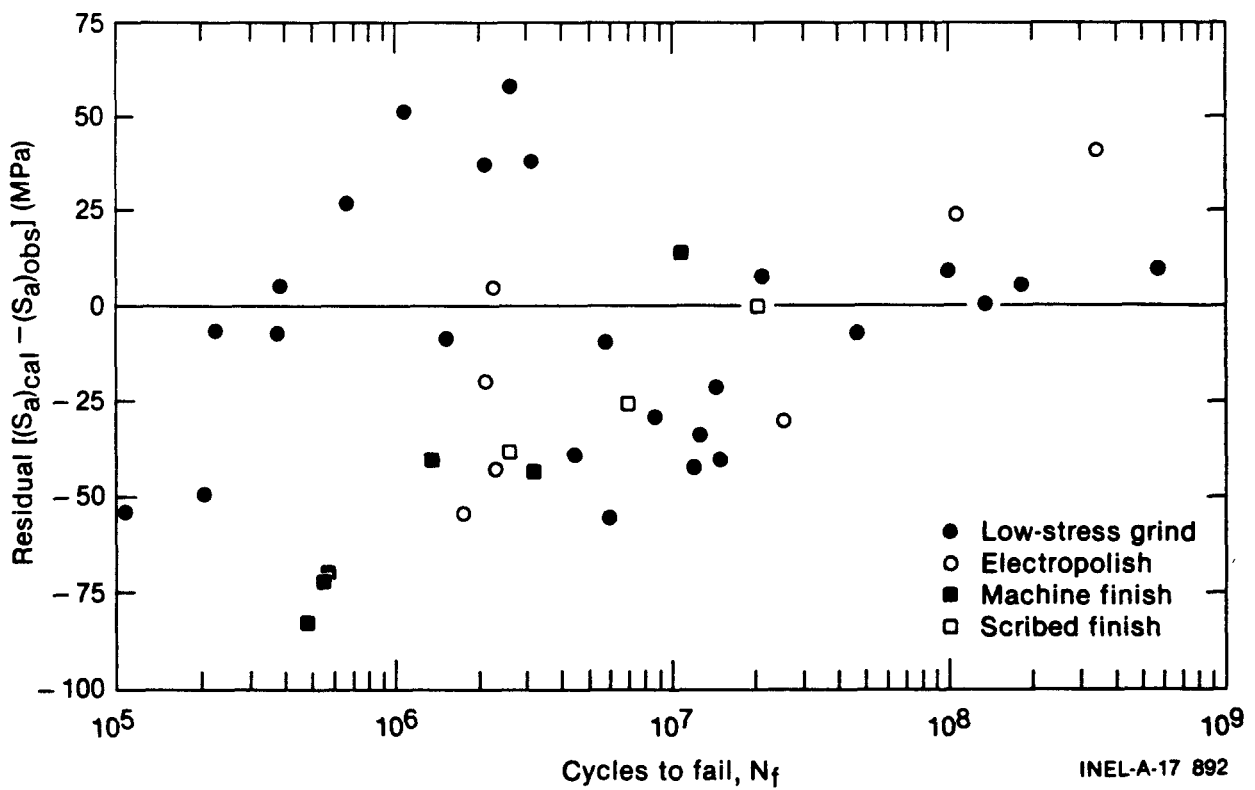


Figure 11. Residuals of curve fit of Alloy 718 plate data at 427°C.

treated and then electropolished to a depth of 0.075 mm did indeed show a near-zero residual stress profile. In the present investigation the round hourglass specimens (5.08-mm minimum diameter) were given a low-stress grind after heat treatment and then electropolished to a depth of 0.075 mm. The attempt was to produce a near-zero surface stress, but it is entirely possible that residual tensile stresses from the grinding operation (see Figure 2) were deeper than 0.075 mm and a compressive stress remained in the final surface to offset the deeper tensile stresses. To resolve the question of why the electropolished specimens in the present study did not exhibit the same reduction in high-cycle fatigue strength as observed in the previous study,³ an actual residual stress profile measurement would be necessary.

The 649°C residuals plot for the tube material is given in Figure 12, wherein the high-cycle fatigue strength is compared for low-stress grind, grit-blast, and belt-sand surfaces. All of the 649°C data were from the tube material. Also, at this test temperature there was no observable difference beyond normal data scatter in the high-cycle fatigue strength of the various surfaces examined

except for two grit-blast tests which fell somewhat below the predicted low-stress grind curve.

CONCLUSIONS

The following conclusions were drawn from the results of this investigation:

1. The residual stress profile that is produced by surface preparation has a greater effect on the high-cycle fatigue strength of Alloy 718 than surface roughness.
2. Surface preparations that are within commercial shop capability, specifically the grit-blast and belt-sand techniques, produce surfaces that are equivalent to carefully prepared low-stress grind laboratory surface finishes with respect to high-cycle fatigue strength.
3. Grain size has a significant effect on the high-cycle fatigue strength of Alloy 718 and may very well be more important than surface-finish methods.

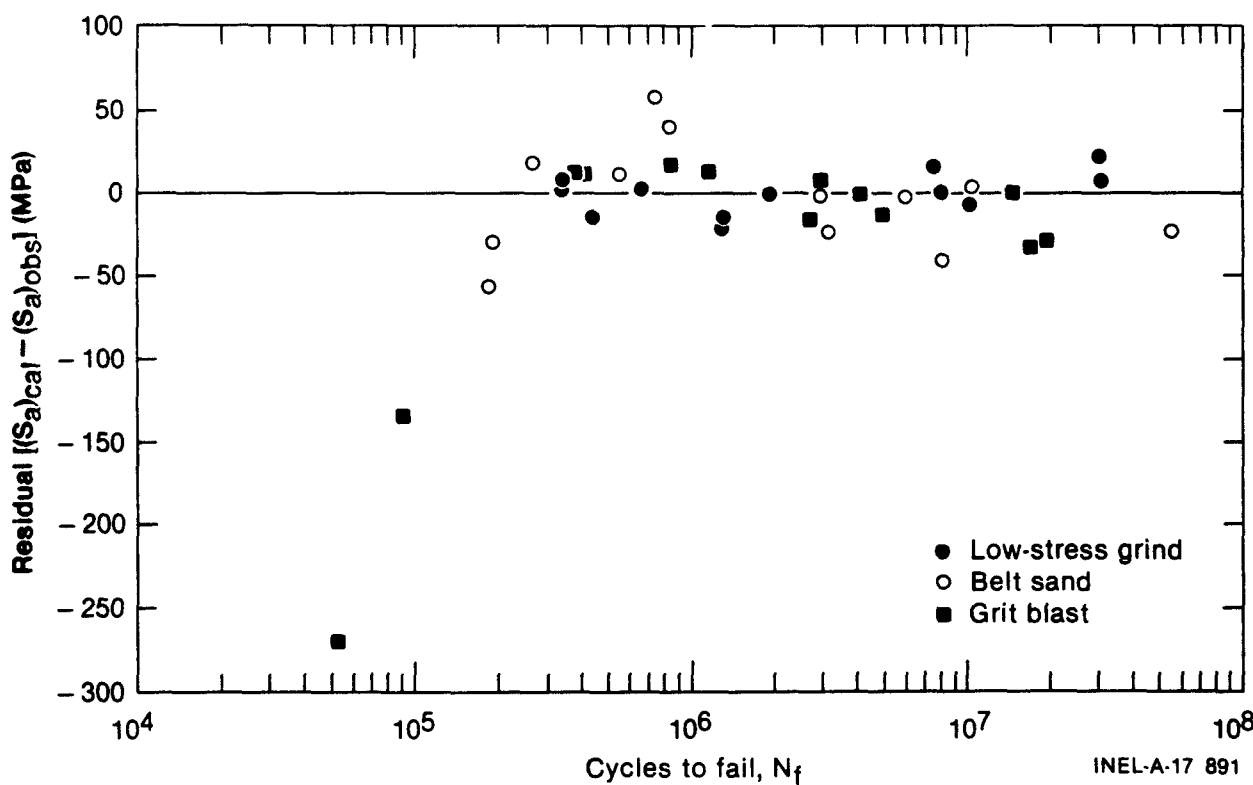


Figure 12. Residuals of curve fit of Alloy 718 tube data at 649°C.

REFERENCES

1. G. E. Korth and G. R. Smolik, *Status of Physical and Mechanical Test Data of Alloy 718*, TREE-1254, March 1978.
2. J. Cammett III and J. B. Kohls, *The Effect of Surface Finishing Treatments on the High Cycle Fatigue Strength of Inconel Alloy 718*, Metcut Report No. 1331-26848, EG&G Purchase Order K-1308, November 21, 1979.
3. W. P. Koster et al., *Surface Integrity of Machined Structural Components*, Technical Report AFML-TR-70-11, AD870146, March 1970, pp. 120-149.
4. W. P. Koster et al., *Manufacturing Methods for Surface Integrity of Machined Structural Components*, Technical Report No. AFML-TR-71-258, AD887105, February 1972, pp. 291-296.
5. *Huntington Alloys*, Inconel Alloy 718 Product Brochure 10M 10-73 T39, 1973.
6. S. O. A. El-Helieby and G. W. Rowe, "Influences of Surface Roughness and Residual Stress on Fatigue Life of Ground Steel Components," *Metals Technology*, June 1980, pp. 221-225.